Utilisation of alkaline electrolysers in existing distribution networks to increase the amount of integrated wind capacity

Mahdi Kiaee [a], David Infield [b], Andrew Cruden [a]

[a] Faculty of Engineering and the Environment, University of Southampton, Room 1036/ Building 23, Southampton, United Kingdom, SO17 1BJ

Phone: +44(0)23 8059 6506, Email: M.Kiaee@soton.ac.uk

[b] Department of Electronic and Electrical Engineering, University of Strathclyde, 204 George Street, Glasgow, United Kingdom, G1 1XW, Phone: +44(0)141548 2373.

Abstract

Hydrogen could become a significant fuel in the future especially within the transportation sector. Alkaline electrolysers supplied with power from renewable energy sources could be utilised to provide carbon free hydrogen for future hydrogen filling stations supplying Hydrogen Fuel Cell Vehicles (HFCV), or Internal Combustion Engines (ICEs) modified to burn hydrogen. However, there is a need to develop and use appropriate strategies such that the technology delivers greater economic and environmental benefits.

In this work, the use of alkaline electrolysers to increase the capacity of integrated wind power in existing radial distribution networks is explored. A novel optimisation approach for sizing, placement and controlling electrolysers has been introduced, and its performance is assessed through modelling using a United Kingdom Generic Distribution System (*UKGDS)* case study. The controller objective is to dispatch alkaline electrolysers appropriately to maximise the total amount of profit from selling hydrogen and reduce the losses within the network while considering the realistic characteristics of pressurised alkaline electrolysis plants and satisfying the power system constraints. The impacts of increasing wind power capacity or the initial size of hydrogen filling stations on the results have been investigated and discussed.

Keywords: Alkaline electrolyser; Renewable power; Active network management; Distribution network; Hydrogen station; Extended optimal power flow

Nomenclature:

$\boldsymbol{\theta}^k$ is the $n_b \times 1$ vector of voltage angles at the time interval of 'k'

ANM Active Network Management

$ASDL$ Aggregate Station Demand Limit (MW)

B The set of bus numbers within the network

C_i Cost function coefficients

$Capital$ The capital cost of an electrolyser in £/MW

D_i^k The amount of demand (excluding the demand of electrolysers) in MW on bus 'i' of the last feeder (from bus 53 to bus 77) at the current time step '*k*'

$\Delta E_{Loss}\%$ The percentage reduction in the total energy loss on the distribution network during the simulation

DER Distributed Energy Resources

DG Distributed Generator

DNO Distribution Network Operator

DSM Demand Side Management

E_{HHV} is the Higher Heating Value (HHV) of hydrogen (39 kWh/kg, [1]).

E_{Loss} Total energy loss during the simulation (MWh)

E_{Loss}^{With} The total energy loss on the distribution network in the system with electrolysers (MWh)

$E_{Loss}^{Without}$ The total energy loss on the distribution network in the system without electrolysers (MWh)

E_{St} The total energy delivered to all of the stations during the simulation (MWh)

55 ELD_{ij}^{k} The demand (MW) of 'i'th active electrolyser located at 'j'th active filling station

56 at the current time step '*k*'

57 *GA* Genetic Algorithm

58 $H2P_{ij}^{k}$ Hydrogen produced by 'i'th active electrolyser located at 'j'th active hydrogen

59 filling station (kg)

60 *HFCV* Hydrogen Fuel Cell Vehicle

61 $\left|I_{ij}^{k}\right|$ The magnitude of current (A) flowing between bus 'i' and 'j' of the power

62 system in the time interval of '*k*'

63 $\left|I_{ij}^{Lim}\right|$ The limit for the current magnitude (A) flowing between bus 'i' and 'j' of the

64 power system

65 *ICE* Internal Combustion Engine

66 k The current time interval number in the simulations

67 $Life$ The lifetime of an electrolyser in years

68 n_b is the number of busses within the network

69 N_{El}^{EST} The number of electrolysers at each station

70 $NAEL_{j}^{k}$ The number of active electrolysers at active filling station 'j' at each time

71 interval '*k*'

72 NAS^{k} The number of active stations at the current time interval of '*k*'

NB The number of branches on the power system

NDP The number of data points during the simulation (e.g. if the simulation is carried out for a duration of 24 hours with time interval of 1 hour, then NDP=24)

NS The total number of filling stations

$\eta_{ij}^{k}\%$ The efficiency of the 'i'th active electrolyser in the 'j'th active station in percentage

NW The total number of wind farms placed within the network

OM The annual operational and maintenance cost of an electrolyser in £/MW/year

OPF Optimal Power Flow

OSZ_i The optimal size of station 'i' in MW

P_g^k is the active power (MW) from slack bus at the time interval of 'k'

$P_{Loss_i}^k$ The amount of power loss (MW) on branch 'i' of the power system at the time interval *'k'*

$P_{Min.El}$ The minimum demand from an electrolyser to stay in active hydrogen production mode, and it is equal to the minimum demand of a station (MW)

$P_{N.El}$ The size (nominal demand) of each electrolysis unit located at each filling station (assumed to be 2 MW here).

Q_g^k is the reactive power (Mvar) from slack bus at the time interval of 'k'

S_{ij}^{k} The complex power flow (MVA) between bus 'i' and 'j' of the network in the current time interval of '*k*'

$\left|S_{ij}^{k}\right|$ The apparent power (MVA) between bus 'i' and 'j' of the power system in the current time interval of *'k'*

$\left|S_{ij}^{Lim}\right|$ The apparent power limit (MVA) between bus 'i' and 'j' of the power system

SD_{i}^{k} The demand (MW) from station 'i' during the current time interval of '*k*'

$\boldsymbol{SD}^{k}$ is the $NS \times 1$ vector of the demand (MW) from stations during the time interval of 'k'

S_{St} The initial size of each station (MW)

$Surplus(k)$ The surplus wind generation (MW)

S_{W}^{i} Size of ith wind farm (MW)

t Metric tonne

T The simulation time interval in hours (In this work T=1 hour)

$TH2P$ The total hydrogen produced in metric tonne (**t**)

$TLB_{Prob}\%$ The probability of thermal limit violations (%)

TLB_{k} The function indicating whether there has been any thermal limit violation within the grid at time interval 'k'

$\boldsymbol{V}_m^k$ is the $n_b \times 1$ vector of voltage magnitudes at the time interval of 'k'

$|V_i^k|$ The magnitude of voltage on bus 'i' of the power system in pu in the current time interval of *'k'*

$|V_i^{Min}|$ The minimum limit for the voltage magnitude on bus 'i' of the power system (pu)

$|V_i^{Max}|$ The maximum limit for the voltage magnitude on bus 'i' of the power system (pu)

$VB_{Prob}\%$ The probability of voltage constraint violation (%)

VB_k The function that indicates whether there has been any voltage violation within the grid at time interval '*k*'

W_i^k The output of wind farm 'i' in MW at the current time step '*k*'

$\boldsymbol{x^k}$ is the optimisation vector at the time step '*k*'

1 Introduction

There is a need to decarbonise the road transportation sector, and there are a number of primary alternatives, such as battery electric vehicles or hydrogen fuel cell vehicles (HFCVs), available for our clean future transport, which can replace the conventional petrol or diesel Internal Combustion Engine (ICE) vehicles. Alkaline

126 electrolysers can be used to produce ‘green’ hydrogen for HFCVs from electricity
127 generated by renewable power resources [2].

128 On the other hand, the global capacity to generate wind power is continuously
129 increasing [3], and the main issue arising from this increase is that the power
130 systems might not be able to absorb the renewable power generated at all times due
131 to lack of demand or breach of power network constraints. Transmission networks
132 are already operating close to their capacity constraints, and adding renewable
133 power generators at transmission level would require upgrading these networks with
134 significant investment, so connecting generation to distribution networks has become
135 more popular. As a result, there is a need to rethink about how to optimally arrange
136 and operate the assets and devices on the distribution networks [4-6].

137 Distributed Energy Resources (DER) are generation technologies (typically
138 renewable generation), energy storage technologies and flexible demand located at
139 distribution level [4]. Current distribution networks have been designed on a ‘fit and
140 forget’ basis, so some technical issues could arise due to adding more distributed
141 renewable generation within the network. Such issues include voltage rises due to
142 the connection of generators or reverse power flows, which could result in the
143 violation of network constraints [7]. Therefore, there is a need to make distribution
144 networks active by inclusion of responsive DER [8].

145 Active Network Management (ANM) techniques operate the network closer to its
146 constraints by real time monitoring and controlling of the network parameters, such

as currents, voltages, Distributed Generator (DG) outputs and responsive or non-responsive load demands, and therefore their utilisation will allow more renewable power resources to be connected to the existing distribution networks while maximising the utilisation of network assets [9]. The current ANM techniques are listed in [9], which also includes load control and energy storage techniques to support increasing renewable power generation.

Different storage devices have been explained and compared in details in [10], [11] and [12], and their applications, advantages and drawbacks are explained in details. The benefits of energy storage devices from the Distribution Network Operator (DNO) point of view are listed below [13].

- Voltage support
- Distribution losses reduction
- Capacity support and deferral of distribution investment

Obviously, in addition to electrolysers, there are other options in the power system, such as batteries, fridges or pumped storage devices, which could be used for Demand Side Management (DSM) purposes, but they are limited, and they are not always available for participating in DSM. The other issue is that they might not be suitable for seasonal storage of electricity. However, hydrogen could be stored for a long period and used as clean fuel in the transportation sector. Therefore, electrolysers should be considered as one of the options to improve the operational performance of the electrical grid, especially, in the case that the grid has a high penetration of variable intermittent renewable power [14].

Most of the published papers in the area of hydrogen production with renewable power [15-19] make the assumption that the wind turbines or photovoltaic cells are physically close to the electrolysers, behind the meter, and they only export electric power to the grid when there is more power available from the renewable sources than can be absorbed by the electrolyser because it exceeds the electrolyser maximum power demand. The point is that in real practical applications the electrolysers, as used in fuel stations for example, are unlikely to be located adjacent to wind farms or photovoltaic generation plants. The situation is very different if they are not on the same bus behind the same meter, as the network operator has to deal with them separately, so there is a need to investigate other scenarios as well. Moreover, the published papers in this area do not address the problem of sizing or placement of electrolysers within power systems. This is an important problem as the benefits of energy storage devices are strictly dependent on their location, sizing and the control strategy to operate them. Importantly, no one has considered the actual measured characteristics of alkaline electrolysers so as to realistically model them in the context of power system operation.

Non-optimal connection of DER could potentially affect the quality of energy supply and damage power system equipment. It can also result in violation of the power system constraints [5]. Therefore, the optimal integration of DER is essential to make sure they would have a positive impact on the network operation. Some optimisation targets, from the DNO perspective, to integrate storage devices within the power system, are listed below.

- Finding the location and number of storage devices.
- Finding the size of storage to minimise capital costs [20].
- Finding the best load of storage during its operation to minimise the losses on the power system while respecting the power system constraints (thermal and voltage limits).
- Maximising renewable power integration.
- Minimising the costs of grid upgrade.

Solving such problem is usually addressed by using multi-objective optimisation methods [21].

Atwa and El-Saadany [22] have proposed a method to allocate energy storage in a distribution system with a significant penetration of wind power to maximise the benefits for the owner of DG and the utility operator. Their strategy tries to size the energy storage devices appropriately to avoid wind power curtailment and minimise the electricity bill. Their analysis compared the annual cost of different energy storage devices considering the total profit for both the utility and the DG owner.

Carpinelli et al. [13] have proposed a new cost-based optimisation strategy for the optimal placement, sizing and control of battery energy storage systems on the power system to provide different services such as loss reduction or reactive power provision. Their strategy minimises the whole system costs while considering the energy storage device profit from price arbitrage.

Celli et al. [21] and Carpinelli et al. [23] have proposed methods to optimally allocate energy storage on the distribution network to reduce losses and defer network upgrades using Genetic Algorithms (GAs). Their method finds the optimal charge and discharge pattern of energy storage devices using inner algorithms based on Dynamic Programming (DP) [21] and Sequential Quadratic Programming (SQP) [23], respectively.

Babacan et al. [24] have also used a Genetic Algorithm (GA) optimization method to reduce the voltage fluctuations caused by PV penetration through deploying battery energy storage systems, then they have conducted sensitivity studies to examine the behaviour of the method under varying sizing costs, siting costs and PV penetrations.

Mehmood et al. [25] have used a genetic algorithm multi-objective optimisation method to find the optimal location and size of battery energy storage systems with a view of increasing the lifespan of the batteries and regulating voltage in a distribution system with wind and solar generators.

Nick et al. [26] have worked on the problem of optimal siting and sizing storage systems within distribution networks to provide voltage support and reduce network losses using GA. Although their technique provides promising results, it is computationally expensive, and due to the non-convex and non-linear nature of the problem, finding the global optimal solution is not guaranteed.

231 An alternative approach to GA is Optimal Power Flow (OPF), which is a technique
232 for optimal operation and planning of power systems [27]. Its aim is to optimise
233 objective functions such as the amount of losses on the power system by setting
234 some control variables in an optimal way while satisfying the demand and grid
235 operating constraints [27]. The extended OPF formulation is a modified version of
236 the standard OPF formulation, which includes additional variables, costs and/or
237 equality and inequality constraints [28]. In this work, the utilisation of extended OPF
238 will be investigated to size, place and control electrolysers in power systems using a
239 heuristic approach to avoid the complications of control strategies that use GAs.

240 The novelty of this work is in the strategy and algorithm used to size, place and
241 control electrolysis hydrogen production stations within a distribution network so as
242 to increase wind power capacity and network asset utilisation. The actual
243 characteristics of pressurised alkaline electrolysers, detailed in [29], are used for the
244 first time to design a realistic control strategy to run them in the power system and
245 find their impact on the electric network. The effectiveness of the proposed strategy
246 is investigated through modelling using *MATLAB* software.

247

248 **2 Methodology**

249 In this section, a number of hydrogen filling stations with electrolysers and wind
250 farms will be added to a feeder of a radial distribution network. It is assumed the
251 electrolysers at the hydrogen filling stations will use some of the surplus wind power

252 from wind farms to produce clean hydrogen for fuel cell vehicles in a future scenario ,
253 e.g. next 20-30 years, where there is a significant penetration of HFCVs with a much
254 more mature and developed hydrogen production and delivery infrastructure.

255 The electrolysers in this system are assumed to be able to change their demands
256 dynamically within their maximum and minimum demand limits. It is assumed that
257 the Distribution Network Operator (DNO) owns and operates the electrolysers, and
258 there is a communication system between the (DNO) and each hydrogen filling
259 station that allows adjustment of their electricity demand. The following optimisation
260 steps are proposed to size, place and control these hydrogen filling stations within a
261 feeder of a radial distribution network so as to maximise the utilisation of grid assets
262 while respecting the power system constraints. The aim is to increase the local wind
263 penetration whilst producing ‘green’ hydrogen for transport using alkaline
264 electrolysers.

265 1. A number of wind farms will be added to a feeder of a radial distribution
266 network without any storage until they breach the power system constraints
267 during the simulation period or require curtailment to meet the constraints.
268 2. A number of filling stations with electrolysers will be added to the same feeder
269 of the network. The stations will have a reasonable distance from each other
270 and they will not be placed on the same buses as wind farms in order to
271 reflect locational constraints. Each filling station will comprise a number of
272 equally sized electrolyser units. The initial aggregate rating of filling stations
273 will be chosen to be close to the aggregate rating of the wind farms. However,

after the simulation the minimum size of stations needed to satisfy the algorithm objectives and constraints will be identified.

3. An extended Optimal Power Flow (OPF) controller with a primary cost function will be used to minimise the electricity demand of the filling stations and distribution losses at each time step while satisfying the power system constraints. The reason to minimise the demand of each station is to minimise the final size (hence the capital costs) of each station. The electrolyser characteristics identified in [29] will be used in the optimisation process. The electricity demand of each station will be determined by the optimisation algorithm, and then the demand of each individual electrolyser making up a station will be determined by a local controller at each filling station.
4. After running the simulation for a duration of a year, the maximum electricity demand of each station during the simulation will be used to determine its optimal rating.
5. The location of the hydrogen stations on the feeder will be varied and then the above steps (3 and 4) will be repeated to find the best solution to minimise the size of stations and network losses while maximising the profit from selling hydrogen according to an ‘income’ function.

Fig. 1 summarises the heuristic optimisation algorithm proposed in this work to size, place and control electrolysis hydrogen filling stations within a radial distribution network.

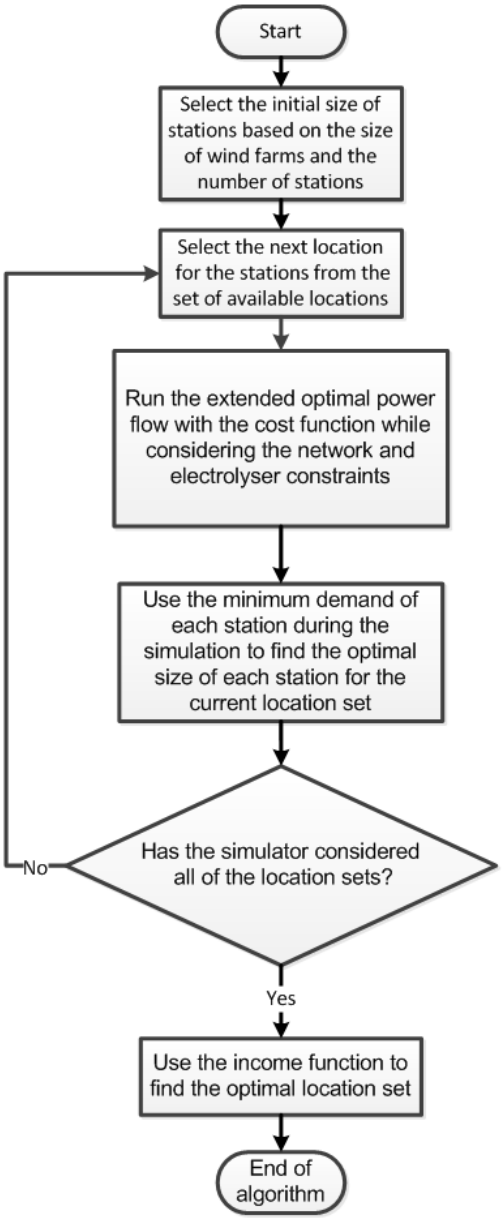

295

296 *Fig. 1 The algorithm used to size, place and control the hydrogen stations*

297 The proposed strategy can also be utilised while placing solar farms in the power

298 system. However, in this work only wind farms are added to the system.

299 It should be noted that the main goal of this work is not to just talk about the benefits
300 of energy storage in the distribution network. The owners of HFCVs have already
301 paid the price of their cars, and that cost is not being paid by the owner of the
302 distribution network or the investors in the filling stations. Therefore, the proposed
303 scenario is very different from the case of just adding storage devices in the power
304 system to improve its performance from both investment and energy efficiency point
305 of views.

306 After the simulation, the results of currents and voltages and distribution losses
307 before and after adding hydrogen filling stations will be compared to assess the role
308 of electrolysers in improving power system operation. In the cases that the voltage of
309 busses or flow of the branches are out of limits, the probability of voltage violations
310 or overload in different scenarios will be compared.

311

312 **3 Modelling details**

313 The United Kingdom Generic Distribution System (*UKGDS*) is a resource for
314 simulation and analysis of the impact of distributed generation on the UK power
315 network. The models represent the most common architectures used by the UK
316 Distribution Network Operators (*DNOs*), but they are slightly altered to facilitate
317 testing and evaluation of new concepts [30].

318 A radial distribution network is used as a case study in this work to evaluate the
319 effectiveness of the proposed strategy. This type of network is used, as it is much

easier to consider the distance of stations from each other while placing them on the network. In real life, it is not very useful to put the filling stations on every node of the power system and then run the optimisation process, which might lead to cases of having some filling stations very close to each other, and on the other hand, having some areas not covered by any nearby hydrogen filling station. Therefore, a radial distribution network will best suit the aim of the work in this work to show the effectiveness of the control strategy. A *UKGDS* phase one High Voltage (*HV*) Underground (*UG*) network [30] is used in this study.

Software was developed by the author using *MATLAB* and *MATPOWER* [28] to simulate the proposed scenarios applied to the *UKGDS* model. Fig. 2 shows the network used in this study, with added hydrogen filling stations and wind farms.

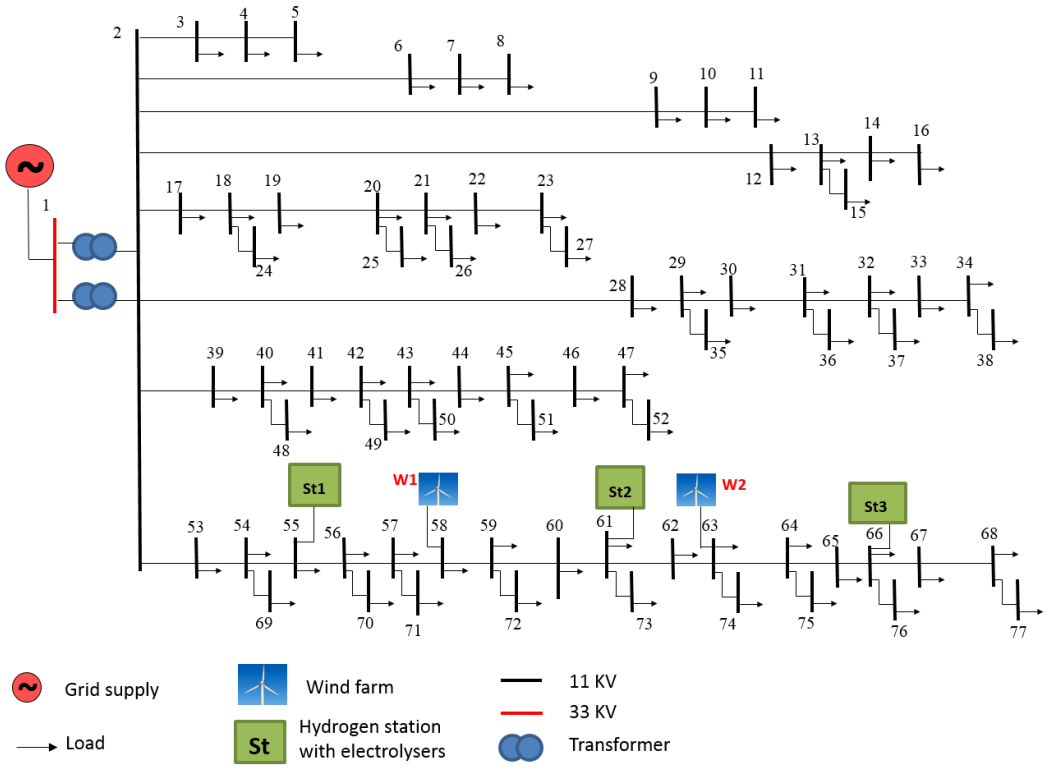

Fig. 2 UKGDS HV UG network with wind farms and hydrogen filling stations

The aggregate total demand on the *UKGDS* HV UG network is 24.2 MW [30], so the electricity demand profile for the United Kingdom [31] is scaled down to match to the load profile of this *UKGDS* system, and then it is used in the simulation process. It is assumed that the loads on each node of the power system are constant during each simulation time interval. The amount of demand at different system nodes is equal to the proportion of loads defined in the *UKGDS* load profile.

In this work, the hydrogen stations and wind farms are modelled on only one feeder of the system (feeder number 8, which is the last one) to assess the performance of the proposed control strategy. The filling stations are added on three buses, and the wind farms are added at bus 58 and 63 of the *UKGDS* model. Table 1 contains the

location of each hydrogen filling station proposed for each simulation scenario. The location of each station in each of the five sets is selected in a way that the stations have a reasonable distance from each other, and they are not placed on the same bus as the wind farms.

Table 1 The location of hydrogen filling stations in each set

Set number/station location	Station bus number		
	Station 1	Station 2	Station 3
Set 1	53	59	64
Set 2	54	60	65
Set 3	55	61	66
Set 4	56	62	67
Set 5	57	64	68

To scale the wind farms to the *UKGDS* model and cause a violation of power system constraints without utilisation of electrolysers, their nominal generation capacity was selected to be 10 MW. Table 2 also shows the location and size of wind farms used in this work.

354 *Table 2 Wind farm location and size*

	Location (bus number)	Capacity (MW)
Wind farm 1	58	10
Wind farm 2	63	10

355

356 Wind speed data with resolution of one hour from two UK regions (Tain Range and
357 Peterhead [32]), which was obtained from the UK meteorological office for the
358 duration of one year, was used in the analysis. For simplicity, it is assumed that the
359 wind turbines used in the wind farms are of the same type and with the same rating,
360 and they have a power curve of a 2 MW wind turbine made by Repower, [33]. Using
361 the wind speed data, the turbine power curve and the rated size of wind farms in
362 Table 2, the output of each wind farm during a year was calculated with a time
363 resolution of one hour.

364 To select the initial size of stations, the following assumptions were made.

365 • The initial size of each station is an integer multiple of 2 MW which is the
366 assumed size of each electrolyser.
367 • The initial size of all the stations are equal (i.e. they have the same number of
368 electrolyser units).

- The aggregate nominal demand of stations is chosen to be as close as possible to the aggregate capacity of wind farms.

Based on these assumptions, the following equation is used to find the initial size of each station (S_{St}) in MW. The 'Round' operator is used to make sure the initial proposed size of each station is an integer multiple of the size of each electrolyser.

$$S_{St} = Round\left(\frac{1}{NS*P_{N.El}} * \sum_{i=1}^{NW} S_W^i\right) * P_{N.El} \quad (1)$$

By inserting the corresponding values in Eq. (1) the initial size of each station was found to be 6 MW.

The number of electrolysers at each station (N_{El}^{EST}) can be calculated from the following equation.

$$N_{El}^{EST} = \frac{S_{St}}{P_{N.El}} \quad (2)$$

This means that 3 electrolysers with a rating of 2 MW are located at each station at the start of the simulation in this first case study.

Two scenarios are considered in the simulations. In the first scenario, the system only has two wind farms without any electrolysers, and the fluctuation in the difference between the local generation and demand must as far as possible be compensated by import/export of power from the distribution substation. In the second scenario, electrolysers are also operating in the system to capture some of the surplus wind power generated within the feeder to alleviate the problems caused

by the distributed wind generation within the network. The assumptions and strategy used in the second scenario to operate the electrolysers is explained below.

It is assumed that the demand of each station is controllable from the distribution network control centre. It is also assumed that each electrolyser behaves like a linear load consuming only active power within its acceptable operational range. The minimum demand of each electrolyser is assumed to be equal to 20% of its nominal demand.

A cost function ($Cost(k)$) is defined to minimise the electricity demand from stations and also the losses within the distribution system.

$$Cost(\mathrm{k}) = C_1 * T * \sum_{i=1}^{NS} SD_i^k + C_2 * T * \sum_{i=1}^{NB} P_{Loss_i}^k \quad (3)$$

The objective of the optimisation is to find the optimisation vector $\boldsymbol{x^k}$, which includes the optimisation variables, to minimise '$Cost$' (£) at each simulation time step.

$$\boldsymbol{x^k} = \begin{bmatrix} \boldsymbol{\theta}^k \\ \boldsymbol{V}_m^k \\ P_g^k \\ \boldsymbol{SD}^k \\ Q_g^k \end{bmatrix} \quad (4)$$

The capital, operational and maintenance (OM) costs, in addition to, lifetime of alkaline electrolyser taken from [34] are used to find C_1 in £/MW/h. It is assumed that annual OM costs of an electrolyser is equal to 2% of its capital costs.

$$C_1 = \frac{Capital}{Life*365*24} + \frac{OM}{365*24} = \frac{1480{,}000}{20*365*24} + \frac{1480{,}000*0.02}{365*24} = 11.82\ (£/MW/h) \quad (5)$$

405 C_2 is the cost of electricity loss and selected to be £35/MWh [35].

406 There are some limits on the demand of stations and power system constraints that
407 should be respected during the optimisation process. Before detailing those limits,
408 some additional variables are defined here.

409 The surplus wind power on the last feeder of the network can be calculated from the
410 following equation. The controller needs to know the amount of wind generation and
411 non-electrolysis demand on each bus of the feeder at each time step in order to
412 calculate the surplus wind generation.

413 $$Surplus(\mathrm{k}) = \sum_{i=1}^{NW} W_i^k - \sum_{i=53}^{77} D_i^k \quad (6)$$

414 If, at a given time step, the surplus power is not sufficient to supply the minimum
415 demand for all of the stations (i.e. to keep at least one of their electrolysers in
416 hydrogen production mode), then the stations with least energy delivered to them up
417 to the current time step will be selected to be removed from list of active stations and
418 their demand will be assumed to be zero. This decision is taken to make sure that
419 the stations which have received more energy during the simulation will be more
420 likely to stay active (produce hydrogen) and continue providing service to improve
421 the performance of the power system, and the stations which have had lower
422 demand in the previous time steps and are more likely to have less impact on the
423 improvement of the results become deactivated when there is not enough surplus
424 power within the system. Fig. 3 shows the algorithm used at each time interval to
425 choose which station is active and which stations do not have any active

electrolysers if the surplus wind power is not sufficient to provide the minimum demand for all of the stations.

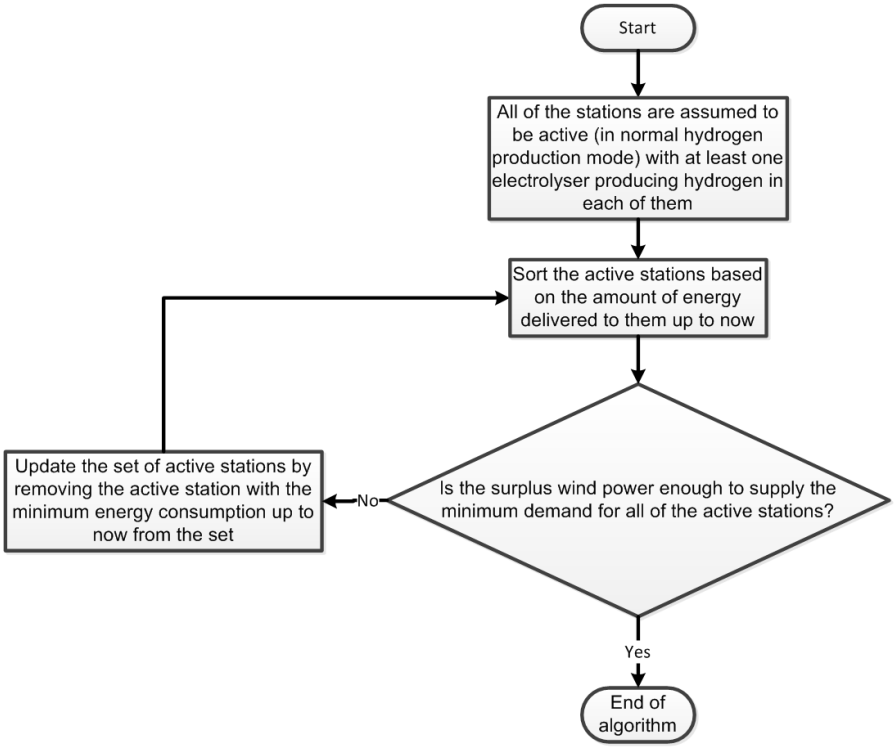

Fig. 3 The algorithm used at each time interval to update the supplied stations (active stations) when there is lack of surplus power for all of the stations

The '$Surplus$' value could become negative at some points when the aggregate wind power generation is below the aggregate local non-electrolysis demand. Therefore another variable called 'Aggregate Station Demand Limit' ($ASDL$) is defined to be used as the limit in the simulations to make sure the aggregate demand from the

436 local hydrogen stations does not exceed the surplus wind (in the case that the
437 surplus wind is positive), and therefore avoid conditions that hydrogen is produced
438 using power from conventional plants, which would introduce unwanted carbon
439 dioxide emissions into the energy supply chain of the hydrogen. In addition, when
440 the '$Surplus$' value is negative, the hydrogen stations should not consume any
441 power.

442 $$ASDL(\mathrm{k}) = \max(Surplus(\mathrm{k}), 0) \quad (7)$$

443 $ASDL$ will always have a non-negative value. This means that if '$Surplus(k)$' is
444 positive then $ASDL(k)$ will be equal to $Surplus(k)$, but if $Surplus(k)$ is negative, then
445 $ASDL(k)$ will be equal to zero.

446 The limits for the aggregate demand of the active stations are defined by the
447 following equation.

448 $$NAS^k * P_{Min.El} \leq \sum_{i=1}^{NS} SD_i^k \leq ASDL(\mathrm{k}) \quad (8)$$

449 The following limit will also be applied to the electricity demand of each active
450 station, as the minimum demand of one station will be equal to the minimum demand
451 of one electrolyser.

452 $$P_{Min.El} \leq SD_i^k \leq S_{St} \quad (9)$$

453 The constraints of the power system should be respected during the optimisation
454 process.

Apparent power constraints:

$$\left|S_{ij}^{k}\right| \leq \left|S_{ij}^{Lim}\right| \quad \forall\, i,j \in B \tag{10}$$

Voltage constraints:

$$\left|V_{i}^{Min}\right| \leq \left|V_{i}^{k}\right| \leq \left|V_{i}^{Max}\right| \quad \forall\, i \in B \tag{11}$$

The voltage variation limits in the *UKGDS* network are ±3% of the nominal nodal voltage, [30]. In this study, the power system limits, taken from [30], are assumed to be constant during the whole year.

After running the simulation and finding the optimal demand of each station at each time step, the distribution network control centre can send the demand set-point of each station to the local station controllers, which are responsible to operate individual electrolysers according to their operational status and constraints. Fig. 4 shows the algorithm used at each time interval to select the number of active electrolysers (electrolysers in hydrogen production mode) and their demand at each active station.

The objective of this algorithm is to keep as many electrolysers as possible in hydrogen production mode to maximise the efficiency of hydrogen production in each filling station. The controller selects the number of active electrolysers ($NAEL_{j}^{k}$) at active filling station 'j' at each time interval *'k'* using the following equation.

$$NAEL_{j}^{k} = \min\left(\left\lfloor \frac{SD_{j}^{k}}{P_{Min.El}} \right\rfloor, N_{El}^{EST}\right) \quad \forall \;\; (1 \leq j \leq \mathrm{NS}\;,\; j \in \mathbb{N}) \tag{12}$$

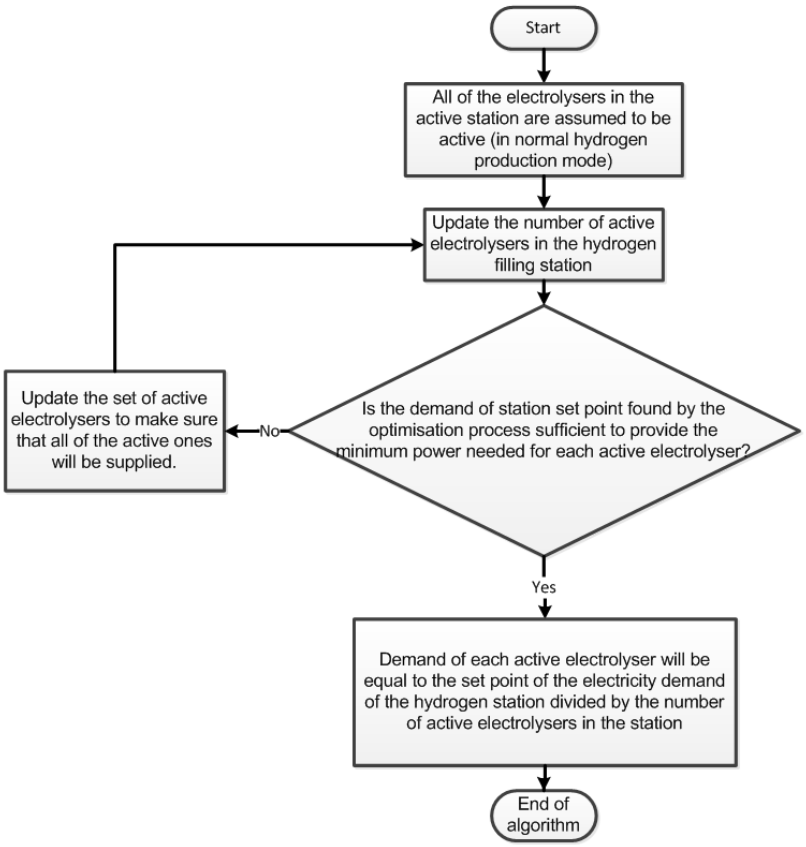

474

475 *Fig. 4 The algorithm used to select the number of active electrolysers and their*
476 *demand at each active station*

477

478 The '$\min$' operator is used to make sure that the number of active electrolysers in
479 each active station at each time interval is not bigger than the total number of
480 electrolysers at each station (N_{El}^{EST}). The 'floor' operator ($\lfloor \quad \rfloor$) is used to make sure
481 that demand set-point of each active station is sufficient to provide the minimum

demand of each active electrolyser located in the station all the time ($NAEL_j^k *$ $P_{Min.El} \leq SD_j^k$).

To calculate the amount of hydrogen production in each station, an efficiency curve must be used for the electrolysers operating at each station. The efficiency curve of electrolysers depend on their design, but to calculate the amount of hydrogen production in this work, it is assumed that all of the electrolysers operating in the filling stations have a linear efficiency curve. These electrolysers have their maximum energy efficiency of 80% when they operate at their minimum demand (20% of nominal demand), and a minimum efficiency of 65% when they are operating at their maximum demand. It is assumed that the efficiency of the rectifier, Faraday efficiency and Balance of the Plant (BOP) of the electrolyser were considered in the electrolyser efficiency curve. In addition, it is assumed that the operating temperature and pressure of the electrolyser will remain constant during the simulation.

The controller gives the same amount of power to each active electrolyser in each station. This means that the hydrogen production system will operate with the maximum efficiency because the electrolysers will consume the minimum possible power at all times. Therefore, the demand of 'i'th active electrolyser (ELD_{ij}^k in MW) located at 'j'th active filling station can be calculated using the following equation.

$$ELD_{ij}^k = \frac{SD_j^k}{NAEL_j^k} \qquad \forall\ (1 \leq i \leq NAEL_j^k\ ,\ 1 \leq j \leq \mathrm{NS}\ ,\ i,j \in \mathbb{N}) \qquad (13)$$

Using the electrolyser efficiency curve and the above equation, the amount of hydrogen produced ($H2P_{ij}^{k}$ in kg) by 'i'th active electrolyser at 'j'th active hydrogen filling station can be found using the following equation.

$$H2P_{ij}^{k} = \eta_{ij}^{k} * \frac{ELD_{ij}^{k} * \mathrm{T} * 1000}{E_{HHV}} \qquad \forall\ (1 \le i \le NAEL_{j}^{k}\ ,\ 1 \le j \le \mathrm{NS}, \quad i,j \in \mathbb{N}) \qquad (14)$$

4 Simulation results and discussions

This section contains the results of running the simulation for a duration of 24 hours and a year using an extended OPF feature in *MATPOWER* implemented in *MATLAB*. For the 24-hour period simulation, the location set 1 is used to show the effectiveness of the control strategy. However, at the end of this section, the results from all location sets, while running the simulation for a year, are presented to identify the best location for the stations.

To achieve the optimisation goal, the algorithm illustrated in Fig. 1 is applied to the system for a 24-hour period with a time resolution of one hour to match the available wind speed data. The other loads in the systems were assumed to be constant during each simulation time interval. The UK electricity demand profile on the 6th of January 2014 is scaled down to *UKGDS* demand scale and used for this simulation.

Fig. 5 shows the demand from the three filling stations within the network during the simulation. The result show that the demand of station 1, which is located at bus 53 (in location set 1), is much lower than the demand of other stations. This means that

522 just two filling stations were able to deal with most of the problems created as the
523 result of adding intermittent renewable power from wind farms, and there was no
524 need to increase the demand of the first station to any significant level to improve the
525 performance of the grid. Therefore, station 1 will have the lowest hydrogen
526 production, and according to the algorithm in Fig. 3 it is more likely to go into standby
527 condition during the simulation if there is lack of wind power generation.

528 Fig. 6 shows the aggregate surplus wind power on feeder 8 and the aggregate
529 demand from all stations. As specified in the control strategy, the aggregate demand
530 of electrolysers is always below or equal to the surplus wind power within the system
531 if this surplus power is a positive value. The difference of power between two curves
532 in Fig. 6 is the power that is exported to other feeders of the power system. In cases
533 where the aggregate surplus power becomes negative or zero, the demand of the
534 filling stations will be zero to avoid the electrolysers working with non-renewable
535 power. In such cases, some limited power will also be imported from the substation
536 to supply some of the local non-electrolysis demands, which were not fully supplied
537 due to lack of local wind power generation.

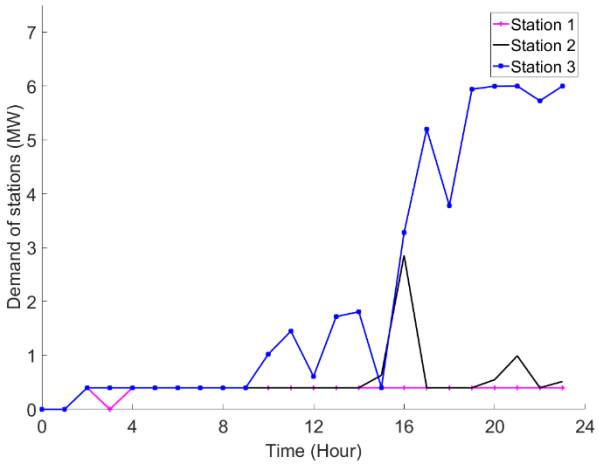

538

539 *Fig. 5 Demand of stations within the network during a 24-hour simulation*

540

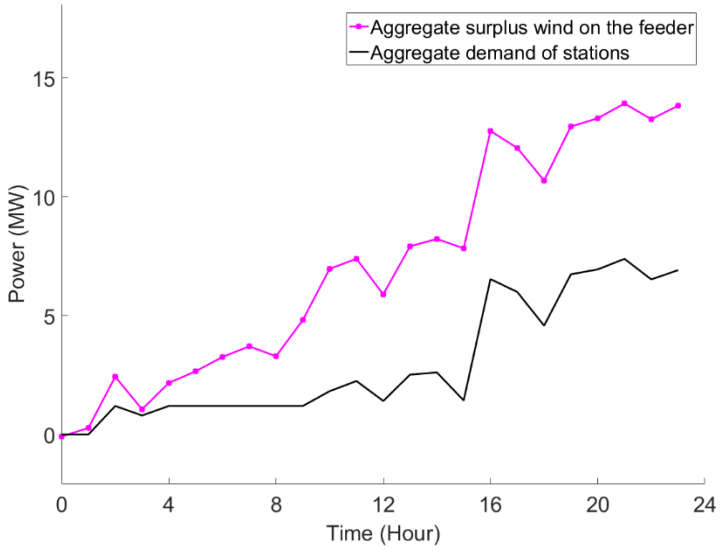

541

542 *Fig. 6 Aggregate surplus wind power and aggregate demand of hydrogen stations*

543

The total amount of wind energy absorbed by the network during the one day was equal to 300.6 MWh, and about 69.4 MWh of energy was used by electrolysers in the filling stations. The rest of the wind energy was consumed by the local demand on the same feeder or the demand on other feeders.

With the introduction of the electrolysers to the system, the voltages on different system nodes change. For example, the voltage on bus 63, which has a nominal voltage of 11KV, is shown in Fig. 7. This bus was selected because it had the maximum voltage rise due to of adding wind farms without the utilisation of electrolysers. As was expected, the maximum voltage rise occurred on one of the buses where wind farms were added to the system. After utilisation of electrolysers, the voltage of the bus remained within the acceptable limits. In addition, the electrolysers smooth the voltage fluctuation on this bus in comparison to the first scenario. The standard deviation of the voltage on this bus without utilisation of electrolysers was 0.0229 pu, which reduced to 0.0056 pu after utilisation of electrolysers during a 24 hour simulation.

The simulation results show that the voltage limit on many buses were breached at least once during the simulation in the system without electrolysers, and that all of them are driven back within the limits as the result of utilisation of the control strategy with electrolysers.

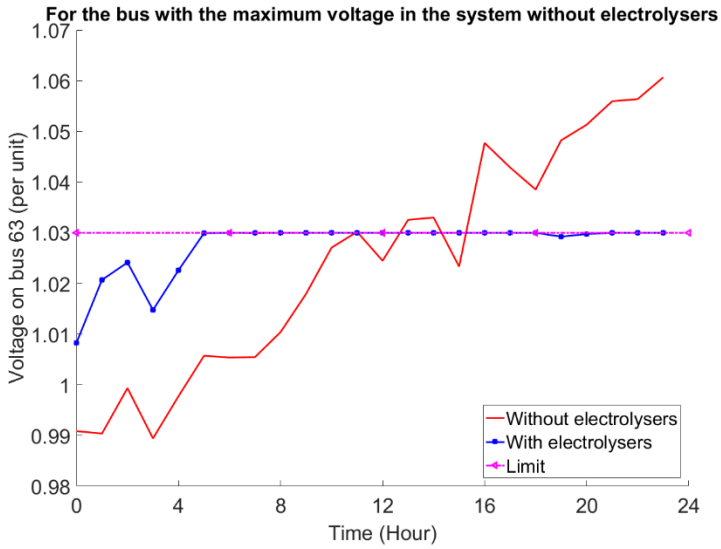

563

564 *Fig. 7 The voltage on bus 63 before and after adding electrolysers to the system*

565

566 Fig. 8 shows the amount of apparent power on the branch of power system, which
567 has the maximum peak value, in percentage terms, without using electrolysers
568 during the simulation. It is obvious that the after using the electrolysers within the
569 system the apparent power of this branch was controlled to remain within the
570 acceptable limits. The simulation results show that the apparent power limit on
571 branches 53, 54, 55, 56, 57 and 58 were breached at least once during the 24-hour
572 simulation in the system without electrolysers, and all of them were driven back
573 within the limits as the result of utilisation of the control strategy with electrolysers.

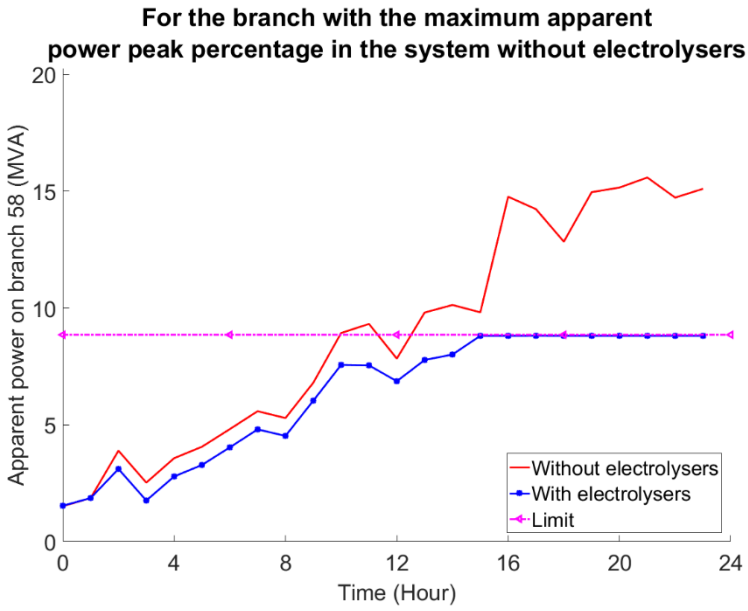

574

575 *Fig. 8 Apparent power on a branch of power system with the biggest peak*

576 *percentage during the simulation*

577

578 On the other hand, there were some branches of the power system, which were
579 underutilised in the system without electrolysers, and their apparent power peak was
580 only a fraction of the nominal capacity limit of the branch. Fig. 9 shows the apparent
581 power of branch 64 of the power system with and without utilisation of electrolysers.
582 It has reached a much higher average apparent power while operating with
583 electrolysers. This shows the effectiveness of the control strategy to increase the
584 utilisation of network assets and to remove the need for grid upgrades and
585 associated costs while respecting the power system constraints and producing
586 'green' hydrogen for the transport sector.

587

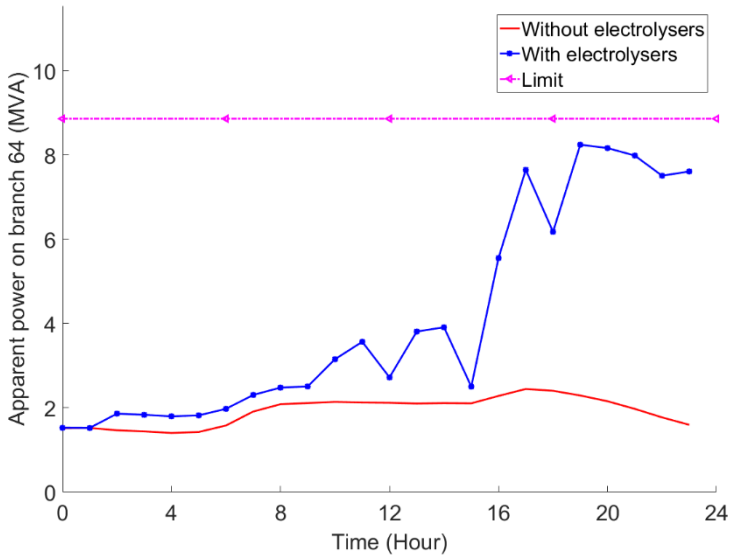

588

589 *Fig. 9 The apparent power of branch 64 of the power system with and without*

590 *utilisation of electrolysers*

591

592 To quantify the probability of constraint violations the following attributes, which were

593 proposed in [36], are used in this work.

594 The probability of voltage constraint violation ($VB_{Prob}\%$) is calculated as the ratio of

595 the total number of time steps that at least one node within the network had a

596 voltage constraint violation divided by the total number of simulation time steps.

597 $$VB_{Prob}\% = \frac{\sum_{k=1}^{NDP} VB_k}{NDP} * 100 \quad (15)$$

598 where

599 VB_k is the function that indicates whether there has been any voltage violation within
600 the grid at time interval *'k'*.

601 $$VB_k = \begin{cases} 0 & if\ (\left|V_i^{Min}\right| \le \left|V_i^k\right| \le \left|V_i^{Max}\right| \quad \forall\, i \in B) \\ 1 & otherwise \end{cases} \tag{16}$$

602 Similarly, the probability of thermal limit violations ($TLB_{Prob}\%$) is calculated as the
603 ratio of the total number of time steps that at least one branch within the network was
604 overloaded divided by the total number of simulation time steps.

605 $$TLB_{Prob}\% = \frac{\sum_{k=1}^{NDP} TLB_k}{NDP} * 100 \tag{17}$$

606 Where TLB_k is the function indicating whether there has been any thermal limit
607 violation within the grid at time interval *'k'*.

608 $$TLB_k = \begin{cases} 0 & if\ (\left|I_{ij}^k\right| \le \left|I_{ij}^{Lim}\right| \quad \forall\, i,j \in B) \\ 1 & otherwise \end{cases} \tag{18}$$

609 These attributes measure the probability of any bus or branch in the system being
610 out of acceptable limits. The probability of a particular bus or branch being out of
611 bounds is equal to or lower than the probability of the system being out of bounds, so
612 such attributes provide a measure of the worst case performance of the system as a
613 whole [36].

614 The one-day simulation results show that the voltage violation and overload
615 probability were 70.83% and 50%, respectively, before adding electrolysers to the

power system. However, after utilisation of electrolysers, those values were found to be zero due to successful enforcement of the constraint limits by the system central controller.

Total energy loss (MWh) during the simulation on the distribution network is calculated using the following equation:

$$E_{Loss} = T * \sum_{k=1}^{NDP} \sum_{i=1}^{NB} P_{Loss_i}^{k} \quad (19)$$

The amount of reduction in the total energy loss on the distribution network during the simulation (ΔE_{Loss}) in MWh can be calculated from the following equation:

$$\Delta E_{Loss} = E_{Loss}^{Without} - E_{Loss}^{With} \quad (20)$$

The percentage reduction in the total energy loss on the distribution network during the simulation ($\Delta E_{Loss}\%$) can be calculated from the following equation:

$$\Delta E_{Loss}\% = \frac{\Delta E_{Loss}}{E_{Loss}^{Without}} * 100 \quad (21)$$

The energy flow from the network to the electrolysers caused a reduction of 5.2 MWh in the total energy loss of the distribution network. This is around 41.5% less than the distribution loss on the system without electrolysers. Despite the fact that the electrolysers act as additional demand on the electrical network, they reduced the distribution losses significantly in this study. The reduction in distribution losses is due to the consumption of some of the surplus power generated by wind farms by

electrolysers on the local feeder, instead of exporting all of the surplus power to other feeders.

After proving the effectiveness of the control strategy during the one-day simulation using set 1 for the location of hydrogen stations, the simulation was run for a duration of one year with time interval of one hour for all of the location sets and the results are included in Table 3. The demand profile of the UK during 2014 [31] was scaled down to match the *UKGDS* demand level and was used for this simulation.

The total hydrogen produced ($TH2P$ in metric tonne (**t**)) during the simulation at all of the electrolysis hydrogen filling stations is calculated from the following equation.

$$TH2P = \sum_{k=1}^{NDP} \sum_{J=1}^{NS} \sum_{i=1}^{NAEL_j^k} H2P_{ij}^k /1000 \quad (22)$$

The total energy (MWh) delivered to all of the stations is calculated from the following equation.

$$E_{St} = T * \sum_{k=1}^{NDP} \sum_{i=1}^{NS} SD_i^k \quad (23)$$

An income function ($Income$) is defined to find the best location set to maximise the amount of hydrogen production and consequently the profit from selling hydrogen while minimising the energy cost of stations, aggregate capital costs of stations, and the total energy loss on the network and during the simulation. The objective is to maximise this income function.

$$\text{Income} = C_3 * TH2P - C_4 * E_{St} - C_5 * \text{NDP} * \text{T} * \sum_{i=1}^{NS} OSZ_i + C_6 * \Delta E_{Loss} \quad (24)$$

Where OSZ_i is the optimal size of station 'i' in MW, and it is determined by the maximum demand of each station during a year simulation.

The first term in 'Income', which is $C_3 * TH2P$, is included to increase the chance of selecting the best answer with the highest hydrogen production. This also increases the chance of selecting the answer with a higher utilisation factor for stations, which will result in more hydrogen production and more profit. C_3 is the selling price of hydrogen (£8/kg or £8000/**t** [37]).

The second term in 'Income', which is $C_4 * E_{St}$, is included to reduce the cost of electrical energy form the function value, and it is also assumed that $C_4 = C_2$. Usually filling station operators who have electrolysers to produce hydrogen can accept electricity from the grid at any time during a day. If an operator agrees to take some of the surplus electricity produced by a wind generator at any time and accepts the peaks and troughs of the received power, then the electricity price for that consumer would fall to a lower price, and it will result in a price reduction of the hydrogen produced by the electrolysers. However, such price reduction is not included in the simulation here.

In this work, it is assumed that $C_5 = C_1$ and $C_6 = C_2$ as both C_1 and C_5 are the coefficients to size stations and C_2 and C_6 are the coefficients for the cost of energy loss on the system.

Considering the proximity to a place with high demand for hydrogen could be added as another optimisation variable, but at this stage, it would need very random

674 assumptions regarding the number of HFCVs visiting the site during the lifetime of
675 each station. In addition, in an operational hydrogen economy, there would be many
676 ways of hydrogen production and delivery, which would again change during the
677 lifetime of each station. It is possible that some of the hydrogen needs of stations
678 would be supplied via other forms of hydrogen production and delivery. If the
679 designer of the system becomes able to forecast the above factors with good
680 accuracy, then they could be added in the optimisation process.

681 Results of Table 3 show that selection of location set 2 will lead to the best result that
682 has the maximum 'Income' value. Interestingly, the percentage of distribution loss
683 reduction for all of the location sets are close to 27%.

684 The final size of some of the stations is found to be lower than 2 MW, inferring that
685 only one electrolyser with a lower nominal demand will be sufficient for those
686 stations. In such cases, the minimum demand of the station will be lower than the
687 initial minimum demand assumed in the control strategy. In addition, for the cases
688 where the final size of a station is not an integer multiple of 2 MW, smaller
689 electrolysers can be used to fill the fraction, although, in practice, the commercial
690 availability of electrolysers would be constrained to limited sizes.

691 The results show that after applying the control strategy, the voltage and apparent
692 power limits were fully within the limits for all of the location sets except set 5. For
693 this last location set, the voltage violation probability was reduced from 72.9% to 0,
694 but the overload probability was reduced from 19% to 1.46% and did not reach zero.

This means that location set 5 is not suitable for electrolysis stations if the power system operator wants to operate electrolysers with the existing network without any grid upgrade or wind power curtailment. However, the reduction of overload probability means that, if there is the possibility to curtail wind power, then it will still less often happen while using the proposed control strategy with location Set 5. The value of 'Income' was also minimum for this location set, emphasising its lack of suitability for the system.

Table 3 Results of a year simulation for different location sets in case study 1

Location set	Set 1	Set 2	Set 3	Set 4	Set 5
$TH2P$ (**t**)	210.3	208.6	207.4	206.5	212.2
E_{St} (MWh)	10,912	10,848	10,789	10,738	11,049
ΔE_{Loss} (MWh)	765.4	757.2	750	747.6	769.9
$\Delta E_{Loss}\%$	27.3%	27%	26.7%	26.7%	27.5%
OSZ_1 (MW)	0.4	0.4	0.4	0.4	6
OSZ_2 (MW)	3.5	2.79	2.76	5.9	6
OSZ_3 (MW)	6	6.0	6.0	6	6

Income (£k)	299.6	363.6	358.7	28	-535.9
$VB_{Prob}^{With}\%$	0%	0%	0%	0%	0%
$TLB_{Prob}^{With}\%$	0%	0%	0%	0%	1.46%

704

705 Despite having the same initial size, the hydrogen stations at different locations had
706 different demand set-points selected by the control strategy, and therefore they had
707 a different final size in the optimised system. It is also not practical to balance the
708 amount of hydrogen produced in the stations with this control strategy, resulting in
709 different amounts of hydrogen production at different stations. Due to implementing
710 the proposed control strategy, a fuel station might have a significantly lower demand
711 in comparison to other stations due to its location during the simulation, meaning that
712 its impact on the improvement of power system operation is very small.

713 One of the advantages of the presented control strategy used in this work is that
714 there is no need to forecast the wind power availability within the system, and it is
715 assumed that the grid control centre can just use the real-time data from the wind
716 power generation units and local demand to calculate the set-point for the demand of
717 each hydrogen station.

718 For the current network used in this work, it takes only 250ms to run the algorithm for
719 each time interval, while using a PC with an Intel Core i7 processor of 3.4GHz and a
720 RAM of 16GB. Execution of a full year simulation takes about 40 minutes for each

721 location set within the UKGDS network. However, full year simulation only needs to
722 be done offline before construction of stations, so it is not necessary to have very
723 small simulation duration.

724 To investigate the impact of initial power rating of filling stations and size of wind
725 farms on the results two more case studies are simulated for a duration of a year,
726 and their results are included in Table 5 and Table 7, respectively.

727 **Case study 2**: The rating of wind farms is unchanged, but the initial size of stations
728 has increased by 50%. Details of this case study are included in Table 4.

729 **Case study 3**: The rating of wind farms is increased by 50%, and as a result, the
730 initial size of stations has increased using Eq. (1). Details of this case study are
731 included in Table 6.

732 As shown in Table 4, the size of wind farms remained unchanged at 10 MW while
733 the initial size of stations is increased from 6 MW in case study 1 to 10 MW in case
734 study 2. The voltage break and overload probabilities have remained unchanged in
735 the system without electrolysers in comparison to case study 1.

736 As shown in Table 5, despite the fact that the maximum final size that the stations
737 were allowed to reach was 10 MW in this case study, the maximum optimal size
738 found is only 7.9 MW. This shows that there is no need to increase the initial size of
739 stations to a very high limit as the optimisation process will try to find the minimum
740 size able to satisfy optimisation objectives.

741

742 *Table 4 Details of case study 2*

Parameter	Value
S_W^i (MW)	10
S_{St} (MW)	10
$VB_{Prob}^{Without}$%	72.9%
$TLB_{Prob}^{Without}$%	19%

743

744 Interestingly, the percentage of distribution loss reduction for all of the location sets
745 has remained close to 27% without significant change in comparison to the first case
746 study. In addition, increasing the initial size of stations did not improve the voltage
747 and thermal limit violation probabilities in location set 5, which had the worst income.
748 The value of income function for all location sets except set 3 are worse in
749 comparison to the first case study. However, the value of income function is bigger
750 for set 3, which is the optimal solution. This means that case study 2 has a slightly
751 better optimal solution in comparison to the first case study. Therefore, it can be
752 recommended that the initial size of stations proposed in the beginning of this paper
753 can be increased by 30% to achieve a better optimal solution. However, if the
754 optimal location set were not available for construction of filling stations using this
755 strategy, then the strategy used in the first case study would be preferred to find the

best size of stations. In addition, adopting this new sizing approach can lead to accepting large gaps between the optimum size of one station and the other ones, i.e. in the results from set 3, the optimal size of station 3 is 7.8 MW while the optimum sizes of other two stations are only 1.1 and 0.4 MW. This is not preferable from practical point of view as it will cause placing one big station and another very small station on the network, and therefore they will have big differences in the amount of hydrogen they produce.

Table 5 Results of case study 2 for a year simulation

Location set	Set 1	Set 2	Set 3	Set 4	Set 5
$TH2P$ (**t**)	216.3	214.7	213.5	212.6	221.5
E_{St} (MWh)	10,911	10,845	10,783	10,730	11,190
ΔE_{Loss} (MWh)	764.7	753.7	744	739.2	781.5
$\Delta E_{Loss}\%$	27.3%	26.9%	26.5%	26.4%	27.9%
OSZ_1 (MW)	0.4	0.4	0.4	0.4	6.9
OSZ_2 (MW)	3	3	1.1	7	7.8
OSZ_3 (MW)	7.9	7.8	7.8	7.7	7

Income (£k)	204.5	200.9	396.4	-220.3	-857.8
VB_{Prob}^{With}%	0%	0%	0%	0%	0%
TLB_{Prob}^{With}%	0%	0%	0%	0%	1.47%

765

766 In case study 3, the size of wind farms has increased to 15 MW and the initial size of
767 stations has also increased to 10 MW according to Eq. (1). As a result, the voltage
768 break and overload probabilities in the system without electrolysers have also
769 increased to 78.9% and 41.4%, respectively.

770

771 *Table 6 Details of case study 3*

Parameter	Value
S_W^i (MW)	15
S_{St} (MW)	10
$VB_{Prob}^{Without}$%	78.9%
$TLB_{Prob}^{Without}$%	41.4%

772

773 As shown in Table 7, the percentage of loss reduction in the system with
774 electrolysers has increased significantly to around 54% in case study 3, due to

injection of a significant amount of wind power to the system during the simulation. In addition, the amount of hydrogen production, energy absorbed by stations, and income have also increased significantly. However, the controller has not been able to satisfy the overload problem completely and just managed to reduce it to 1% during the simulation for most of the location sets. The highest amount of income function in this case study belongs to location set 5. However, the overvoltage and overload probabilities were rather higher and equal to 2.42% and 16.7%, respectively, for this location set. Obviously, the system operator cannot add unlimited capacity of wind farms and electrolysers to the system expecting that the controller should achieve the power system constraint limits. If more wind farms were added to the system, then they would generate more power, and more electrolysers could be added to the network to absorb this extra energy. However, the power system operator should make sure that the network limits would not be violated due to adding extra wind power capacity or electrolysis demand.

Table 7 Results of case study 3 for a year simulation

Location set	Set 1	Set 2	Set 3	Set 4	Set 5
$TH2P$ (**t**)	601.9	597.4	593.9	589.7	674.7
E_{St} (MWh)	32,143	31,906	31,711	31,450	36,881

ΔE_{Loss} (MWh)	3145.9	3,078	3,013	2,964	3,210
$\Delta E_{Loss}\%$	55.2%	54%	52.9%	52.1%	56.4%
OSZ_1 (MW)	8.4	8.4	8.5	8.6	10.2
OSZ_2 (MW)	10	10	10	10	10.5
OSZ_3 (MW)	8.2	8.2	8.1	8.6	7.1
Income (£k)	1036.9	1005.1	981.5	898.8	1335.3
$VB_{Prob}^{With}\%$	0%	0%	0%	0%	2.42%
$TLB_{Prob}^{With}\%$	1%	1%	1%	1%	16.7%

5 Conclusions

In this work, a novel approach that uses an extended OPF was proposed to size, place and control pressurised alkaline electrolysers located at hydrogen filling stations to increase the amount of wind power generation capacity within an example radial distribution network while satisfying the power system constraints and electrolyser characteristics. Simulation results show the effectiveness of the proposed control strategy to maintain the power system parameters within acceptable limits, while directing some of the surplus power to the electrolysers to produce 'green' hydrogen. The proposed strategy increases the network asset

801 utilisation while deferring the need for network upgrade investment for the integration
802 of more intermittent wind power.

803 Three cases were investigated in this work. In the first case study, which represented
804 the main strategy, the initial size of filling stations were selected based on the main
805 strategy proposed in the work. The simulator was easily able to find the optimal
806 solution, which resulted in completely satisfying the voltage and thermal limit
807 constraints during one year simulation.

808 In the second case study, the size of wind farms was unchanged, but the initial size
809 of fuel stations were increased by 50%. The optimal location set resulted in a slightly
810 better income of £396.4k instead of £363.6k during the one-year simulation.
811 However, it is found that adopting the new initial sizing approach in the second case
812 study can lead to large gaps between the optimum sizes of one hydrogen filling
813 station compared with the other ones.

814 In the third case study, the size of wind farms was increased by 50%, and as a
815 result, the initial size of fuel stations was increased according to Eq. (1). Due to this
816 change, as was expected, the amount of hydrogen production and the income also
817 increased significantly. However, the extended OPF strategy was not able to fully
818 solve the overload and overvoltage problems during all of the time steps for the
819 optimal location set. For other non-optimal location sets, which have lower income,
820 the voltage constraints were satisfied, but the overload probability reduced to 1%.
821 This proves that, if we combine this control strategy with wind power curtailment

schemes, then we would be able to increase the integrated wind power capacity within the system significantly by only curtailing the wind power during 1% of the time.

It is financially and technically viable to use alkaline electrolysers to produce clean fuel for future transportation needs and, at the same time, use them as dynamic load to improve the performance of power system while absorbing the additional power generated by variable renewable resources. Such electrolysers can provide long-term energy storage and provide load control on a short-term basis.

Acknowledgements

Funding: This work was supported by the UK Engineering and Physical Sciences Research Council (EPSRC) as part of the SUPERGEN project on 'Delivery of Sustainable Hydrogen (DoSH2)' [grant reference: EP/G01244X/1].

References

[1] Summary of electrolytic hydrogen production, National Renewable Energy Laboratory, http://www.nrel.gov/hydrogen/pdfs/36734.pdf, 2004.

[2] Hosseini SE, Wahid MA. Hydrogen production from renewable and sustainable energy resources: Promising green energy carrier for clean development. Renewable and Sustainable Energy Reviews. 2016;57:850-66.

[3] Ellabban O, Abu-Rub H, Blaabjerg F. Renewable energy resources: Current status, future prospects and their enabling technology. Renewable and Sustainable Energy Reviews. 2014;39:748-64.
[4] Pepermans G, Driesen J, Haeseldonckx D, Belmans R, D'haeseleer W. Distributed generation: definition, benefits and issues. Energy Policy. 2005;33:787-98.
[5] Integration of Distributed Generation into the UK Power System, Distributed Generation and Sustainable Electrical Energy Centre website, http://www.sedg.ac.uk/Publication/DGSEE%20Integration%20of%20DG%20Mar2007.pdf, 2007.
[6] Saint-Pierre A, Mancarella P. Active Distribution System Management: A Dual-Horizon Scheduling Framework for DSO/TSO Interface Under Uncertainty. IEEE Transactions on Smart Grid. 2017;8:2186-97.
[7] Plecas M, Gill S, Kockar I, Anderson R. Evaluation of new voltage operating strategies for integration of distributed generation into distribution networks. 2016 IEEE PES Innovative Smart Grid Technologies Conference Europe (ISGT-Europe), 2016, 1-6.
[8] Lopes JAP, Hatziargyriou N, Mutale J, Djapic P, Jenkins N. Integrating distributed generation into electric power systems: A review of drivers, challenges and opportunities. Electric Power Systems Research. 2007;77:1189-203.
[9] Liew SN, Strbac G. Maximising penetration of wind generation in existing distribution networks. IEE Proceedings in Generation, Transmission and Distribution. 2002;149:256-62.
[10] Barton JP, Infield DG. Energy storage and its use with intermittent renewable energy. IEEE Transactions on Energy Conversion. 2004;19:441-8.
[11] Zhao H, Wu Q, Hu S, Xu H, Rasmussen CN. Review of energy storage system for wind power integration support. Applied Energy. 2015;137:545-53.
[12] Ferreira HL, Garde R, Fulli G, Kling W, Lopes JP. Characterisation of electrical energy storage technologies. Energy. 2013;53:288-98.

871 [13] Carpinelli G, Celli G, Mocci S, Mottola F, Pilo F, Proto D. Optimal Integration of
872 Distributed Energy Storage Devices in Smart Grids. Smart Grid, IEEE Transactions
873 on. 2013;4:985-95.
874 [14] Gutiérrez-Martín F, Confente D, Guerra I. Management of variable electricity
875 loads in wind – Hydrogen systems: The case of a Spanish wind farm. International
876 Journal of Hydrogen Energy. 2010;35:7329-36.
877 [15] Hug W, Bussmann H, Brinner A. Intermittent operation and operation modeling
878 of an alkaline electrolyzer. International Journal of Hydrogen Energy. 1993;18:973-7.
879 [16] Brossard L, Bélanger G, Trudel G. Behavior of a 3 kW electrolyser under
880 constant and variable input. International Journal of Hydrogen Energy. 1984;9:67-72.
881 [17] Zhou T, Francois B. Modeling and control design of hydrogen production
882 process for an active hydrogen/wind hybrid power system. International Journal of
883 Hydrogen Energy. 2009;34:21-30.
884 [18] Pino FJ, Valverde L, Rosa F. Influence of wind turbine power curve and
885 electrolyzer operating temperature on hydrogen production in wind–hydrogen
886 systems. Journal of Power Sources. 2011;196:4418-26.
887 [19] Bergen A, Pitt L, Rowe A, Wild P, Djilali N. Transient electrolyser response in a
888 renewable-regenerative energy system. International Journal of Hydrogen Energy.
889 2009;34:64-70.
890 [20] Fernández-Blanco R, Dvorkin Y, Xu B, Wang Y, Kirschen DS. Optimal Energy
891 Storage Siting and Sizing: A WECC Case Study. IEEE Transactions on Sustainable
892 Energy. 2017;8:733-43.
893 [21] Celli G, Mocci S, Pilo F, Loddo M. Optimal integration of energy storage in
894 distribution networks. PowerTech, 2009 IEEE Bucharest, 2009, 1-7.
895 [22] Atwa YM, El-Saadany EF. Optimal Allocation of ESS in Distribution Systems
896 With a High Penetration of Wind Energy. IEEE Transactions on Power Systems.
897 2010;25:1815-22.
898 [23] Carpinelli G, Mottola F, Proto D, Russo A. Optimal allocation of dispersed
899 generators, capacitors and distributed energy storage systems in distribution

networks. Modern Electric Power Systems (MEPS), 2010 Proceedings of the International Symposium, 2010, 1-6.
[24] Babacan O, Torre W, Kleissl J. Siting and sizing of distributed energy storage to mitigate voltage impact by solar PV in distribution systems. Solar Energy. 2017;146:199-208.
[25] Mehmood KK, Khan SU, Lee SJ, Haider ZM, Rafique MK, Kim CH. Optimal sizing and allocation of battery energy storage systems with wind and solar power DGs in a distribution network for voltage regulation considering the lifespan of batteries. IET Renewable Power Generation. 2017;11:1305-15.
[26] Nick M, Hohmann M, Cherkaoui R, Paolone M. Optimal location and sizing of distributed storage systems in active distribution networks. IEEE Grenoble PowerTech 2013, 2013, 1-6.
[27] Bamane PD, Kshirsagar AN, Raj S, Jadhav H. Temperature dependent Optimal Power Flow using gbest-guided artificial bee colony algorithm. International Conference on Computation of Power, Energy, Information and Communication (ICCPEIC 2014), 2014, 321-7.
[28] Zimmerman RD, Murillo-Sanchez CE, Thomas RJ. MATPOWER's extensible optimal power flow architecture. Power & Energy Society General Meeting, 2009 (IEEE PES 09), 2009, 1-7.
[29] Kiaee M, Cruden A, Chladek P, Infield D. Demonstration of the operation and performance of a pressurised alkaline electrolyser operating in the hydrogen fuelling station in Porsgrunn, Norway. Energy Conversion and Management. 2015;94:40-50.
[30] United Kingdom Generic Distribution System (UKGDS), Defining the Generic Networks, DTI Centre for Distributed Generation and Sustainable Electrical Energy, http://www.sedg.ac.uk/, 2005.
[31] National grid website, http://www.nationalgrid.com/uk/Electricity/Data/Demand+Data/, 2014.
[32] Hill DC, McMillan D, Bell KRW, Infield D. Application of auto-regressive models to U.K. wind speed data for power system impact studies. IEEE Transactions on Sustainable Energy. 2012;3:134-41.

[33] REpower Systems website, http://www.repower.com/de/, 2014.
[34] Ulleberg Ø, Nakken T, Eté A. The wind/hydrogen demonstration system at Utsira in Norway: Evaluation of system performance using operational data and updated hydrogen energy system modeling tools. International Journal of Hydrogen Energy. 2010;35:1841-52.
[35] The Balancing Mechanism Reporting System (BMRS) website, http://www.bmreports.com/bsp/SystemPricesHistoric.htm, 2013.
[36] Alarcon-Rodriguez AD. A multi-objective planning framework for analysing the integration of distributed energy resources [PhD thesis]. University of Strathclyde: University of Strathclyde; 2009.
[37] ITM power website, http://www.itm-power.com/news-item/hydrogen-cost-structure-update, 2015.